Evaluating the land-surface component of NWP models using field experiment data, specifically BOREAS.

Alan K. Betts
(and many co-authors)

58 Hendee Lane
Pittsford VT 05763

akbetts@aol.com

ECMWF/WCRP/GEWEX Workshop

29 June - 2 July 1998

1. INTRODUCTION

The direct comparison between field experiment time-series data and model data from near-by grid-points in data assimilation and forecast systems has proved very useful in identifying systematic errors in the model physical parameterizations (Betts et al., 1993; 1996a,b, 1997, 1998a,b,c,d), and in developing improved model parameterizations (Viterbo and Beljaars, 1995; Hong and Pan, 1996; Chen et al., 1996). Primarily these comparisons identify physical processes, which are represented poorly or not represented at all in the models. This review is based on an evaluation (Betts et al, 1998c) of the reanalysis models (Kalnay et al, 1996; Gibson et al, 1997) from the National Centers for Environmental Prediction and National Center for Atmospheric Research (NCEP/NCAR) and European Centre for Medium-Range Forecasts (ECMWF) over grassland and the boreal forest. Here we will just show the boreal forest comparison using data for 1996 from the Boreal Ecosystem-Atmosphere Study (BOREAS) old black spruce site at 55.879°N, 98.484°W near Thompson, Manitoba. There are some physical aspects of the northern boreal forest, which are not represented in the reanalysis models, which we will illustrate with data from Betts et al (1998d).

2. COMPARISON OVER THE BOREAL FOREST

In this section we will compare 1996 data from the BOREAS old black spruce site, 40 km west of Thompson, Manitoba (designated TF-3 for tower flux site 3; Goulden et al, 1997), with the NCEP/NCAR reanalysis and the 1996 ECMWF operational model. Black spruce, a wetland conifer, is the dominant species of the boreal landscape in this area, covering about 50% of the area (Barr et al, 1997). Although there are other landscape "types" (deciduous aspen, dry conifers including jack pine, mixed stands, as well as lakes and fens), we do not yet have a landscape surface flux average, so we will use this black spruce time-series for illustration and as a reference. Evapotranspiration from both the black spruce and the other coniferous species is low in the boreal forest, considerably lower than the total evaporation in the global forecast models. In Spring and early summer the lakes are cooler than the air, and evaporation from them is also small. The boreal landscape has frozen soil and is covered by snow about half the year. Neither the albedo with snow under the trees, nor the effect of frozen soil is represented properly in the global reanalyses. Both models have consequently large errors in Spring, when incoming solar radiation is high, but the ground is still frozen and there is snow under the canopy. The NCEP/NCAR data (from May to October, 1996) is from that reanalysis, but the ECMWF data is from the closest grid point in the 1996 T-213 operational model, which has the same land surface model as their reanalysis model (since the ECMWF reanalysis is not available for 1996). Not only is the spacial resolution higher, but we have for each day an hourly time series from a 24-h short term forecast from 1200 UTC, instead of 3-hourly values. However, as we shall compare chiefly daytime means, this higher temporal resolution is not significant here. We shall contrast in some Figures

some additional data from the March 1997 ECMWF model to show the impact of changes in the snow albedo introduced in late 1996 in the operational model.

2.1 Spring over the boreal forest.

Figure 1 shows day-time (1200-2400 UTC) net radiation from March 1 to June 10, 1996 from the data and the ECMWF model, and the NCEP/NCAR reanalysis from May 1. The data (solid line) show steadily rising R_{net} with maxima in April (Day 92-121) in the range 300-400 Wm^{-2}. In contrast the ECMWF model, R_{net} is <100 Wm^{-2} in April. The error here is caused by the use of a grassland snow albedo of 80% in the model, while in the boreal forest, the snow under the canopy is largely shaded, and the albedo is typically <20% (Betts and Ball, 1997). The snow 'melts' in the ECMWF model in the first week of May, and R_{net} climbs to values comparable to the observations.

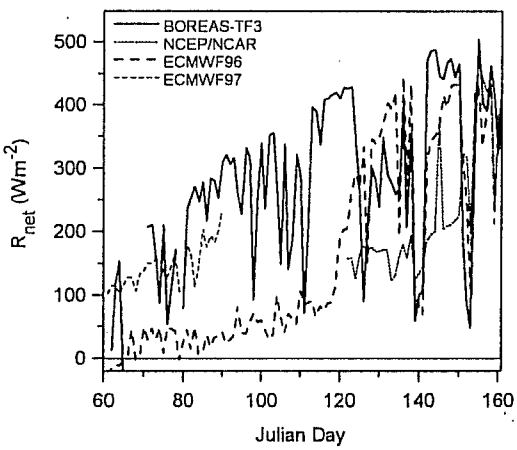

Figure 1. R_{net} comparison with BOREAS TF3 black spruce site in Spring, 1996.

The NCEP/NCAR reanalysis has a similar error, as it generally has an albedo of 60% with snow. The snow in this model does not melt till late May (actual snowmelt near Thompson was middle to late May), so we see values of R_{net} <200 Wm^{-2} during most of May (Day 122-152).

The light dashed curve is from the ECMWF model for the following year, March 1997, after the forest snow albedo was corrected in the operational model in December 1996 to a more reasonable boreal forest landscape average of 20%. This has clearly improved the estimate of R_{net} : the model value is still below that observed, but this is consistent with the fact that the albedo of this spruce site is significantly lower than 20%. The boreal landscape contains lakes and fens, and deciduous species as well as spruce and pine forests. Both summer and winter, the spruce canopies have a lower albedo (Betts and Ball, 1997) than the other vegetated sites. The lakes have a low albedo in summer and a high albedo in winter, when frozen and snow-covered.

This albedo error has a huge and very important impact on the *SH* flux in Spring, as seen in Figure 2 (as well as on BL depth and lower tropospheric temperatures). By late March, the observations show daytime (1200-2400 UTC) averaged *SH* fluxes above 200 Wm^{-2} on sunny days, while the ECMWF model *SH* flux is near zero. After snow 'melts' in the ECMWF model, the *SH* flux rapidly climbs (days 120-130). In the NCEP/NCAR reanalysis the *SH* also stays near zero till snowmelt, and has some large excursions of

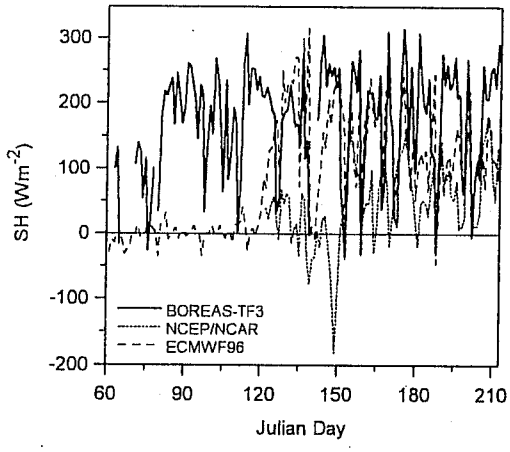

Figure 2. BOREAS daytime sensible heat flux comparison from March to July, 1996.

downward *SH* flux (day 149) associated with the snowmelt itself. (The ECMWF model, in contrast, which has a separate snow analysis, and does not have a self-consistent budget for the solid water phase, uses very little energy for the melt phase). The impact of these *SH* flux errors in the reanalyses is very large. Deep BL's are seen over the boreal forest in Spring (Betts et al, 1996b), driven by the large *SH* fluxes, as evaporation remains small before the ground melts. The models in contrast have low *SH* fluxes, and cannot develop deep BL's in Spring. This leads to large systematic errors in 5-day forecasts of lower tropospheric temperature (as large as -5K at 850 mb in March, April means over Eastern Russia in the ECMWF analysis (see Viterbo and Betts, 1997). Because the error involves a deep BL and extensive regions of forest, it has a global impact on the model high latitude systematic errors. Figure 2 extends till the end of July. On sunny days, the *SH* flux at this spruce site

remains generally higher than in the ECMWF model and much higher than in the NCEP reanalysis.

Figure 3 shows the *LH* flux comparison. The observations show very low *LH* flux until May 20, and then, as the soil and snow melt, average sunny day values in late May are around 100 Wm^{-2}. The ECMWF model has low fluxes in early 1996 before snowmelt (for the wrong reason, as R_{net} is very small: see Figure 1), and then values climb and are generally above those observed. The dashed data from March 1997, after the snow albedo has been reduced to 20%, shows that, although the model R_{net} is improved (Figure 1), the new 1997 operational model now gives too high *LH* fluxes in March (and consequently its corresponding *SH* flux is still biased low).

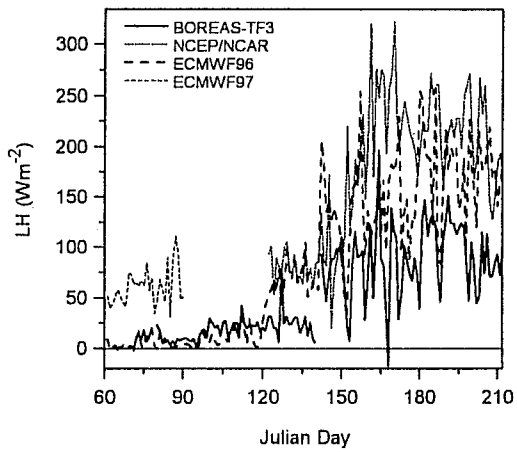

Figure 3. As Figure 2 for latent heat flux.

This is because the model evapotranspiration algorithm is unaware of the frozen soil. The NCEP/NCAR reanalysis (dotted), even with the low values of R_{net} in May gives too high evaporation, and evaporation climbs steadily in late May after snow melt, reaching values over 250 Wm^{-2} in early June. Such large values were seen in BOREAS only over aspen forests. Clearly there is room for improvement in both models both in the formulation of the snow albedo for forests, and the evaporation algorithms, which need to be aware of frozen ground at these high latitudes. Insufficient attention has been paid to the proper representation of forest albedo with snow in global forecast models. Accurate global observational studies of forest albedo with snow under the canopy are needed. The reduction of the boreal forest snow albedo in the operational ECMWF model to 20%, in December 1996, while simple, is a clear improvement, but the evaporation in winter and Spring now appears high.

2.2 Boreal forest fluxes in June and July.

We will now look at the fluxes after snowmelt, and after the thaw of the upper layers of the soil (which occurs at different times for different landscape types (Betts et al, 1996b)). After snow-melt (late May in Thompson), the R_{net} comparison between models and data improves (not shown). In June and July, both models generally have a larger *LH* flux and a smaller *SH* flux than the spruce site (Figures 2 and 3). Figure 4 compares daytime (1200-2400 UTC) *EF* (upper curves) and precipitation (lower curves) for the period after snowmelt to the end of July. Observed daytime average *EF* remains quite low at the black spruce site all Summer.

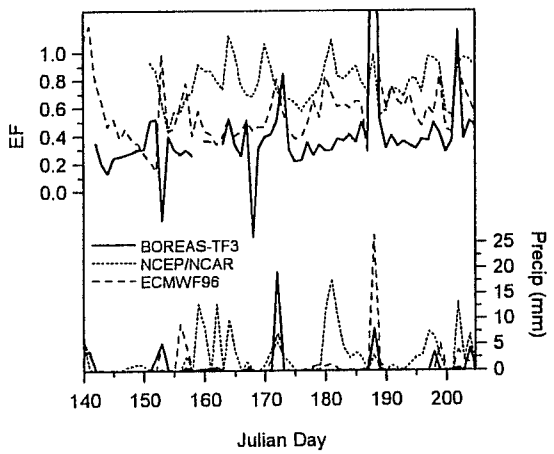

Figure 4. Summer evaporative fraction.

(The spikes generally correspond to days of low fluxes). Typically the ECMWF model has a higher *EF* and the NCEP/NCAR reanalysis is higher still, particularly in June when the surface stays near saturation. We see that the NCEP/NCAR reanalysis has some spurious rainfall peaks (as over the FIFE site, not shown). The reason appears to be the same: namely the model BL stays nearly saturated all day with a high θ_E, and rain persists. One consequence is that the *SH* flux stays low during these rainfall events in the NCEP/NCAR reanalysis and evaporation stays high. For the BOREAS northern study area, deciduous species and fens, which have a much higher *EF* than the black spruce, cover less than 20% of the area. Thus even without a proper landscape average for comparison, it seems likely that evaporation in the global models is too high in early summer. The tight stomatal control over evaporation by the forest is not well represented in the models. The agreement between the ECMWF model and the data over the boreal forest is not nearly as good as over the FIFE

grassland (Betts et al, 1998c)). In Figure 9, from day 142 to 151, we see the steady fall of *EF* in the ECMWF model, as the soil moisture falls in the absence of rain; much like the behaviour at the FIFE site in late July (Betts et al, 1998a,c). However the boreal spruce forest (where *EF* is primarily biophysically controlled) does not behave in this way at all. The data (solid line) show a small fall after the rain, probably as the moss layer dries out (Betts et al., 1998d), but *EF* then recovers and increases slowly, as the soil has just melted, and water is presumably more available to the trees. Clearly further developments are needed to represent well the physiological controls of the boreal forest on evaporation over the season.

3. Observed physical controls on evaporation at the black spruce site.

We will now extract some figures from Betts et al 1998d, showing the important processes that can be seen in the time-series of fluxes at the old black spruce site from 1994-1996. This analysis focuses on linking the forest energy and water fluxes to surface and atmospheric variables. We calculated a bulk "vegetative resistance" R_{veg} (the reciprocal of a conductance) from measured evaporation and a near-surface meteorological model, similar to that used in the ECMWF model. From a climatic perspective, it is this additional resistance to evaporation at the surface that distinguishes the land surface from the ocean, and gives the deeper, drier boundary layers seen over land.

3.1 Dependence of evaporation on season

Figure 5 shows the seasonal cycle of daytime (a 1200-2400 UTC mean) R_{net}, *SH*, *LH*, and the residual (heavy solid line), and the night-time R_{net} and residual (a 0000-1200 UTC mean). All the data has been simply binned into months. There is a sharp fall in the daytime residual between May and June coinciding with the end of snow and soil melt. Simultaneously, the daytime *LH* flux rises after soil melt, coinciding with the increase in plant photosynthetic activity; while *SH* rises much earlier in Spring, when R_{net} is high and evaporation low.

Figure 6 shows latent heat *(LH)* plotted against incident photosynthetically active photon flux density *(PPFD)*, with a breakdown of the data into the three broad seasonal classes. The data has been simply averaged in 300 μmol $m^{-2}s^{-1}$ bins centered on the values shown.

In this summer data set, a mean *PPFD* of 1650 μmol $m^{-2}s^{-1}$ corresponds to near-full sun at local

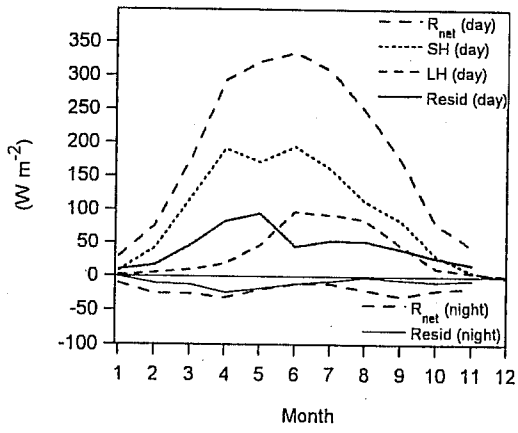

Figure 5. Annual cycle of terms in the surface energy balance.

noon and a mean R_{net} of about 590 Wm^{-2}. We show some representative standard deviations: they are quite large as the meteorological parameters vary, in addition to the sampling error in each 30-min mean. Spring *LH* flux, when the soil is frozen, is very low and increases little with *PPFD*. Consequently at high radiation levels, the *SH* flux is high, which leads to deep boundary layers over the forest in Spring. The *LH* flux in Fall after frost and its dependence on *PPFD*, while larger than in the Spring, is considerable less than in summer.

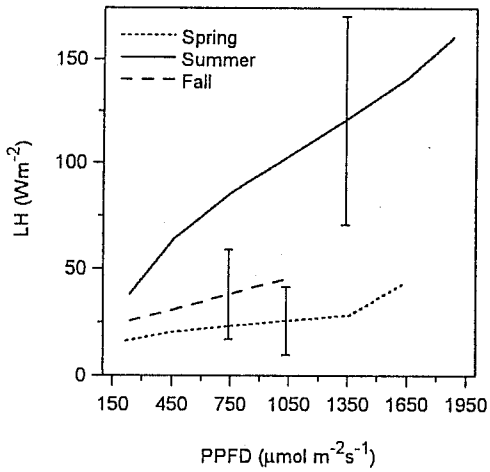

Figure 6. Dependence of LH on incident photosynthetically active photon flux density (PPFD) for Spring (frozen ground), Summer and Fall (after frost).

3.2 Dependence of R_{veg} on PPFD and RH

Figure 7 shows both R_{veg} (left hand scale) and average vegetative conductance, g_{veg} , on right

hand scale, for three light levels, binned by *RH*. At high humidities, g_{veg} increases rapidly, while R_{veg} has a quasi-linear dependence on *RH*. The effect of this strong dependence of R_{veg} on *RH* shown in Figure 7 is that evaporation is very *insensitive* to *RH*.

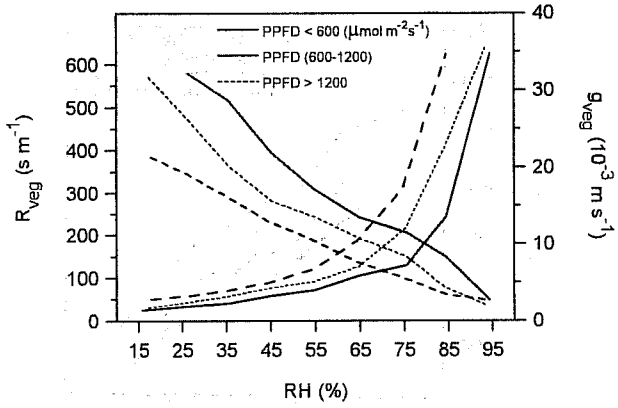

Figure 7. R_{veg} (left hand scale) and vegetative conductance (g_{veg} : right hand scale), for three light levels, binned by RH.

Figure 8 shows *LH* as a function of *RH* for different light levels for the summer data, showing this weak dependence. It appears that the forest has a tight physiological control on its transpiration rate, so that evapotranspiration *does not increase as RH goes down*.

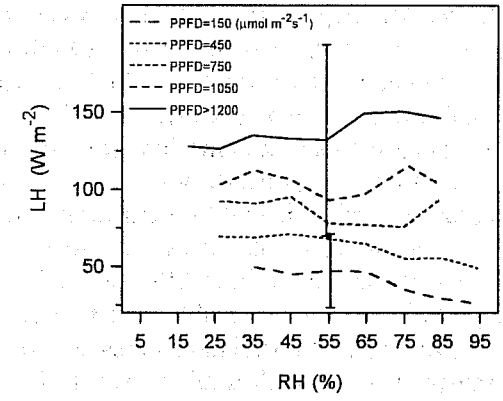

Figure 8. LH as a function of RH for different light levels, showing weak dependence

3.3 Dependence on wet surface index.

Figure 9 shows how R_{veg} for the forest system is a strong function of a wet surface index, related to the days after rain (Betts et al, 1998d). The solid curve corresponds to a dry surface, and the dashed and dotted curves to higher wet surface indices (WS = 5 means 5mm of rain fell the day before). When the surface is wet, the mean "vegetative resistance" is more than halved at higher *RH* (in fact the evaporation from the wet moss is not stomatally controlled) . The corresponding *PPFD* distribution (not shown) is quite similar across all wet surface indices, so this is not an effect of different light levels.

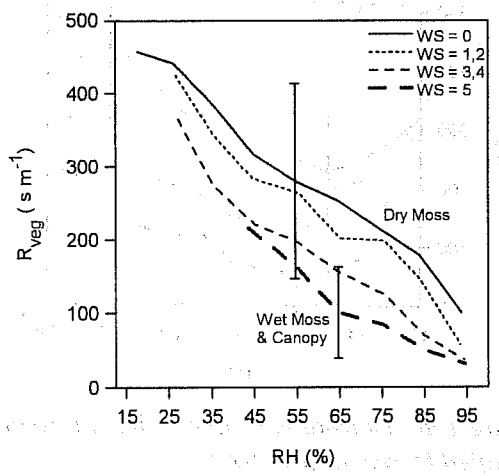

Figure 9. R_{veg} for the forest system in summer as a function of RH and wet surface index.

3.4 Diurnal variation as a function of wet surface index, and feedback to the BL.

Figure 10a illustrates the large diurnal variation of R_{veg}. There is a mid-morning minimum of R_{veg} (a consequence of *RH* falling and *PPFD* rising), and a late afternoon maximum for all values of the wet surface index (local noon is 1800 UTC). With a wet surface index = 5, the computed mid-morning "vegetative resistance" is a *factor of four* lower than when the moss is dry. This is a larger difference between wet and dry surfaces than in Figure 9, because the mean *RH* is much higher on days with a wet surface. Evaporative fraction at local noon increases uniformly from only 0.3 for the dry surface days to 0.5 for the wet surface index of 5 (not shown).

As over grassland sites (Betts and Ball 1995, 1998), this large difference in the surface resistance to evaporation (which leads to a difference in *EF*) directly influences the mean diurnal cycle of *RH*, and consequently the lifting condensation level (*LCL*). Figure 10b shows the diurnal cycle of P_{LCL}, the pressure height to the *LCL* of near-surface air (at 29m), stratified by wet surface index. A uniform decrease of *LCL* (and with it mean cloud-base) with increasing surface wetness is visible. The mean *LCL* is over 100 hPa lower on the subset of days when the surface is very wet. This is the important climatic mechanism by which the resistance to evaporation from the surface feeds back on the BL depth and the

convective cloud field. It has no parallel over the ocean, where water is freely available for evaporation.

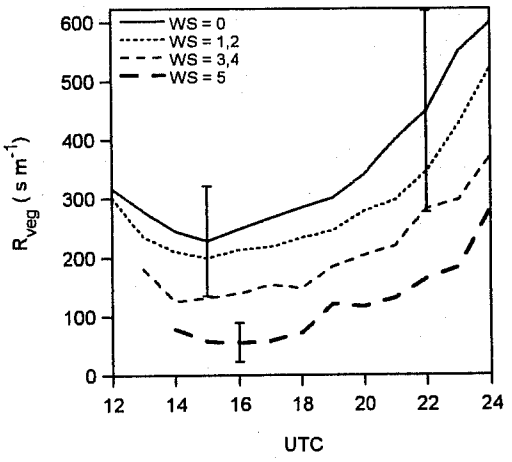

Figure 10a. Diurnal variation of R_{veg} in summer, stratified by wet surface index.

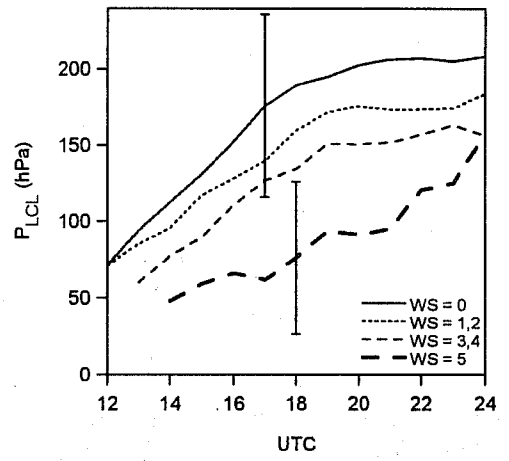

Figure 10b. Diurnal cycle of P_{LCL}, the pressure height to the LCL, stratified by wet surface index.

A small part of the P_{LCL} differences in Figure 10b can be attributed to decreases in the incoming photosynthetic radiation, which falls from 1370 $\mu mol\ m^{-2}\ s^{-1}$ to 970 $\mu mol\ m^{-2}\ s^{-1}$ at local noon as the wet surface index increases from 0 to 5, presumably because cloud cover increases.

3.5 Dependence on Cloud cover

Figure 11 shows the further stratification of R_{veg} from Figure 7c using the cloud index into sunny (CX=0: dotted) and cloudy (CX=1: solid) sky conditions (representing direct and diffuse solar radiation), for two ranges of *PPFD*. R_{veg} is less at all relative humidities under cloudy skies by about 50 s m^{-1}. Our regression analysis in section 5 will confirm this. This is consistent with the findings of Goulden et al. (1997) that photosynthetic uptake is greater under cloudy skies at the same radiation level, because the diffuse radiation penetrates the canopy more efficiently. The forest transpiration is thus higher when the incoming radiation is diffuse.

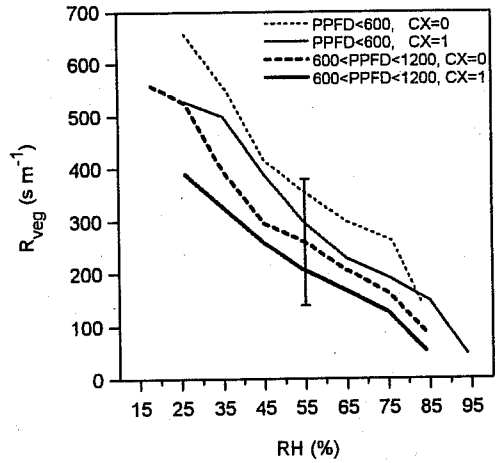

Figure 11. Dependence of R_{veg} on cloud index in two PPFD ranges.

4. Conclusions

We have analyzed the surface energy balance over a boreal spruce forest using three years of 30-min averaged data, collected during the 1994-1996 BOREAS experiment, 40 km west of Thompson, Manitoba, and the two reanalysis models to highlight the processes which appear important from a climatic perspective. The physical processes that are apparent in the data are a useful guide to their representation in model parameterizations of the boreal forest in climate and weather forecast models. The seasonal cycles of the surface sensible and latent heat differ markedly at these high latitudes. The sensible heat flux rises rapidly in Spring as solar radiation increases, while evapotranspiration is small until the soil melts in May. The residual in the energy balance (we have no measurements of ground storage) has a marked seasonal as well as diurnal dependence. In spring when the ground and snow is melting, the residual reaches 30% of daytime net radiation.

Our results are representative of only a single site, but the physical dependencies they show for this dominant vegetation type in the boreal forest provide a semi-quantitative check on forest vegetation models used in weather forecast and climate models. Some global forecast models, such as those at ECMWF and NCEP (National Centers for Environmental Prediction), do not represent all the dependencies that are clearly apparent in the

data. The seasonal dependence, especially the effect of frozen soil in Spring is of particular climatic importance, as is the large impact of the surface water storage reservoir on evaporation (which has been noted by other BOREAS investigators: Price et al, 1997). In addition, some vegetation parameterizations do not include the large *RH* dependence seen here in the data, which acts to stabilize the *LH* flux from the forest, across a wide range of conditions. The lower vegetative resistance under cloudy skies, which is apparent in the data, could also be of climatic significance.

Acknowledgments.

Alan Betts acknowledges support from the National Science Foundation under Grant ATM-9505018, from the NOAA Office of Global Programs under Grant NA76GP0255, from NASA under Grant NAG5-7377 and from ECMWF for travel.

References.

Barr, A.G. A.K. Betts, R. Desjardins and J. I. MacPherson, Comparison of regional surface fluxes from boundary-layer budgets and aircraft measurements above boreal forest. *J. Geophys. Res., 102*, 29213-29218, 1997.

Betts, A.K. and J.H. Ball, The FIFE surface diurnal cycle climate. *J. Geophys. Res. 100*, 25679-25693, 1995.

Betts A. K. and J. H. Ball, Albedo over the Boreal forest. *J. Geophys. Res., 102*, 28901-28909, 1997.

Betts A. K. and J. H. Ball, FIFE surface climate and site-average data set: 1987-1989. *J. Atmos Sci., 55*, 1091-1108, 1998.

Betts, A.K., J.H. Ball, and A.C.M. Beljaars, Comparison between the land surface response of the European Centre model and the FIFE-1987 data. *Q. J. R. Meteorol. Soc., 119*, 975-1001, 1993.

Betts, A.K., S-Y. Hong and H-L. Pan, Comparison of NCEP/NCAR Reanalysis with 1987 FIFE data. *Mon. Wea. Rev., 124*, 1480-1498, 1996a.

Betts, A. K., J.H. Ball, Beljaars, A.C.M., M.J. Miller and P. Viterbo, The land-surface-atmosphere interaction: a review based on observational and global modeling perspectives. *J. Geophys. Res., 101*, 7209-7225, 1996b.

Betts, A. K., F. Chen, K. Mitchell and Z. Janjić, Assessment of land-surface and boundary layer models in 2 operational versions of the Eta Model using FIFE data. *Mon. Wea. Rev., 125*, 2896-2915, 1997.

Betts, A. K., P. Viterbo and A.C.M. Beljaars, Comparison of the ECMWF reanalysis with the 1987 FIFE data. *Mon. Wea. Rev., 126*, 186-198, 1998a.

Betts, A. K., P. Viterbo and E. Wood, Surface Energy and water balance for the Arkansas-Red river basin from the ECMWF reanalysis. *J.Clim.* (In press, 1998b).

Betts A. K., P. Viterbo, A.C.M. Beljaars, H-L. Pan, S-Y. Hong, M. L.Goulden and S.C. Wofsy, 1998c: Evaluation of the land-surface interaction in the ECMWF and NCEP/NCAR reanalyses over grassland (FIFE) and boreal forest (BOREAS). *J. Geophys. Res.* (In press)

Betts, A. K., M. L. Goulden and S. C. Wofsy, Controls on evaporation in a boreal spruce forest. *J. Clim.*, (conditionally accepted, 1998d).

Chen, F.,K. Mitchell, J. Schaake, Y. Xue, H-L. Pan, V. Koren, Q. Duan, and A. Betts, Modeling of land-surface evaporation by four schemes and comparison with FIFE observations. *J. Geophys. Res., 101*, 7251-7268, 1996.

Gibson, J. K., P. Kallberg, S. Uppala, A. Nomura, and E. Serrano, ERA description, ECMWF Reanalysis Project Rep. Series, *1*, ECMWF, Reading , United Kingdom, 72pp, 1997.

Goulden, M.L., B.C. Daube, S.-M. Fan, D.J. Sutton, A. Bazzaz, J.W. Munger, and S.C. Wofsy, Physiological Responses of a Black Spruce Forest to Weather, 1997. *J. Geophys. Res.*, **102**, 28987-28996.

Hong, S-Y. and H-L. Pan, Implementing a nonlocal boundary layer vertical diffusion scheme for the NCEP Medium-Range forecast model. *Mon. Wea. Rev., 124*, 2322-2339, 1996.

Kalnay, E. and Coauthors, The NCEP/NCAR 40-year Reanalysis Project. *Bull. Amer. Meteor. Soc., 77*, 437-471, 1996.

Price, A. G., K. Dunham, T. Carleton and L. Band, 1997: Variability of water fluxes through the black spruce (*Picea mariana*) canopy and feather moss (*Pleurozium schreberi*) carpet in the boreal forest of Northern Manitoba. *J. Hydrol.*, **196**, 310-323.

Viterbo, P. and A.C.M. Beljaars, An improved land-surface parameterization in the ECMWF model and its validation. *J. Clim., 8*, 2716-2748,1995.

Viterbo P., and A.K. Betts, The forecast impact of changes to the snow albedo of the boreal forests. CAS/JSC Working Group on Numerical Experimentation. #25., "Research Activities in Atmospheric and Oceanic Modeling, 1997.